Line shape and composition of the In $3d_{5/2}$ core-level photoemission for the interface analysis of In-containing III-V semiconductors

J. Mäkelä[a,*], M. Tuominen[a], M. Kuzmin[a,b], M. Yasir[a], J. Lång[a], M.P.J. Punkkinen[a], P. Laukkanen[a,*], K. Kokko[a], K. Schulte[c], J. Osiecki[c], R.M. Wallace[d,*]

[a]*Department of Physics and Astronomy, University of Turku, FI-20014 Turku, Finland*
[b]*Ioffe Physical-Technical Institute, Russian Academy of Sciences, St. Petersburg 194021, Russian Federation*
[c]*The MAX IV laboratory, P. O. Box 118, Lund University, SE-221 00 Lund, Sweden*
[d]*Department of Materials Science and Engineering, The University of Texas at Dallas, Richardson, Texas 75080, USA*

Abstract

The In $3d_{5/2}$ photoelectron spectroscopy peak has been widely used to determine the interface structures of In-containing III-V device materials (e.g., oxidation states). However, an unclear parameter affecting the determination of the energy shifts and number of the core-level components, and therefore, the interpreted interface structure and composition, is still the intrinsic In $3d_{5/2}$ peak line shape. It is undecided whether the line shape is naturally symmetric or asymmetric for pure In-containing III-V compounds. By using high-resolution photoelectron spectroscopy, we show that the In $3d_{5/2}$ asymmetry arising from the emission at high binding-energy tail is not an intrinsic property of InAs, InP, InSb and InGaAs. Furthermore, it is shown that asymmetry of In $3d_{5/2}$ peaks of pure III-V's originates from the natural surface reconstructions which cause the coexistence of slightly shifted In $3d_{5/2}$ components with the symmetric peak shape and dominant Lorentzian broadening.

Keywords: Line shape, III-V semiconductor, Photoelectron spectroscopy, Interfacial analysis

1. Introduction

The goal of utilizing atomic-scale knowledge and control of the surface/interface properties of III-V crystals (e.g., GaAs, InAs, InGaAs, InN, InP, InGaSb) have become more and more essential for III-V applications (e.g., detectors, laser diodes, solar cells, transistors) via the development of nanoscale III-V materials for the devices. Toward that target, one of the most utilized methods has been the element-sensitive core-level photoelectron spectroscopy (CLPES), which provides irreplaceable information about several phenomena occurring at the surfaces and interfaces (in the range of nanometers). These include intrinsic properties, such as shifts and line shape differences in the energy levels of the elements due to the surface reconstruction causing variations in electronic environments and also extrinsic properties such as changes in surface chemistry and backgrounds in the spectra arising from plasmon excitations

---

*Corresponding author. Address: Department of Physics and Astronomy, University of Turku, FI-20014 Turku, Finland. Tel: +358 2 333 6659 (P. Laukkanen)

Email addresses: `jaakko.m.makela@utu.fi` (J. Mäkelä), `pekka.laukkanen@utu.fi` (P. Laukkanen), `rmwallace@utdallas.edu` (R.M. Wallace)

and scattering in the sample medium. Such spectral differences are helpful in the studies of physical and chemical properties, for example, structure and composition of the semiconductor interfaces. For identifying and attributing the features of the measured spectra correctly, it is essential to have rigorous reference measurements and/or calculations of pure elements and compounds.

The chemical states of indium are of particular importance in the analysis of III-V compound semiconductor interfaces. Indium is present in various semiconductor device applications, such as III-V surface channel metal oxide semiconductor field effect transistors (MOSFETs) [1–7] and solar cells [8–10]. The In 3d spectra have been widely used in the studies of these materials and the associated interfaces [1–6, 11–16] because In 3d has a large spin-orbit split (~7.5 eV), allowing detailed analysis of single peaks (i.e., $d_{5/2}$ and $d_{3/2}$). Furthermore, the alternative In 4d emission of the InGa-containing compounds is often complicated by the overlapping Ga 3d emission [17, 18]. The In 3d peaks of metallic samples often show a tail-like distribution of photoelectrons on the high binding-energy (BE) side due to secondary electron excitations [17, 18] (i.e., asymmetric line shape), which appears to be absent in the spectra of In-containing oxides. For In-containing III-V's, both asymmetric and symmetric, along with tail-compensating additional Voigt shaped In 3d peaks have been used in the fitting procedure [1–4, 11–16]. This issue significantly affects CLPES conclusions, for example, in the establishment of the presence of interface or environment-induced changes in the In bonding configuration. The fitting is further complicated by the issue that low oxidation states of In can cause only slight shifts (around +0.5 eV) relative to the emission from bulk-like III-V crystal. In this study, we have measured and analyzed the In 3d spectra of atomically clean InAs(100), InP(100), InSb(100) and $Ga_{0.5}In_{0.5}As$(100) surfaces. The findings clearly support that the high binding-energy tail of the In 3d peaks is not an intrinsic property of III-V crystals, and that the previously proposed reconstruction models cause the coexistence of slightly shifted, symmetric In $3d_{5/2}$ peaks, which explains the In 3d spectra for these semiconductors.

2. Experimental

2.1. Sample treatments and measurements

Experiments were performed at the MAX-lab (Lund) synchrotron radiation center. Clean semiconductor surfaces were obtained by performing cycles of Ar-ion sputtering ($1 - 5 \times 10^{-6}$ mbar, 15 mA, 1 kV, around 45° angle to surface) and post heating (for 15 to 30 min) in ultrahigh vacuum (UHV) at 400–500 °C. After several (4 to 8) such cycles, low-energy electron diffraction (LEED) showed sharp (4×2) patterns for InAs(100) and InSb(100) as well as (2×4) pattern for InP(100). For InGaAs(100), only one heating at 450 °C and cleaning cycle was needed to observe (4×2) reconstruction because the substrate piece was As-capped. The normal emission spectra were measured on the beamline I311 with an instrumental resolution of about 0.15 eV. An energy interval of 0.02 eV for each data point was used except for InAs a more rough 0.05 eV.

Table 1: Fitting parameters for the studied In 3d$_{5/2}$ bulk and SCLS emission peaks. Slightly different positions and FWHMs were acquired for measurements between different photon energies. SCLS positions are adjusted to reconstruction-induced values reported earlier [19, 20]. All of the values are given in eV. SCLS and metallic In positions are given relative to the bulk peak.

| | Bulk | | SCLS | | Metallic In | |
	FWHM	position	FWHM	positions (relative to bulk)	FWHM	position
InAs	0.33–0.40	444.04–444.09	0.47–0.53	c(8×2) ζa: -0.16, -0.09, +0.10, +0.27, +0.30	-	-
InP	0.30–0.31	444.23–444.40	0.38–0.51	(2×4): -0.40, -0.15, -0.10 -0.07, +0.11, +0.15	0.53–0.73	443.68–443.85
InSb	0.30–0.50	443.95–444.02	0.43–0.50	c(8×2) ζ: -0.29, -0.10, +0.07 +0.17, +0.26, +0.30, +0.36	-	-

2.2. Peak fitting

A combination of a linear and Shirley background was subtracted from the In 3d$_{5/2}$ spectra using an interval of 3.5–4.0 eV. For low photon energies and hence low electron kinetic energies, a more linear (up to 80 % linear, 20 % Shirley) background subtraction was used to take the rapid rise of background of low kinetic energy electrons into account. For high photon energies, a less linear (down to 50 % linear, 50 % Shirley) was used. Different background-subtraction approaches did not significantly change the results presented below.

To analyze the asymmetric vs. symmetric nature of the In 3d line shape, we first tested fitting of the In 3d$_{5/2}$ emissions with only one component/peak. In these fittings, the Gaussian and Lorentzian type contributions were allowed to vary and optimal parameters were obtained. The Voigt approximation peaks were constructed from the Lorentzian and Gaussian peak shapes' product with the fractions of each as follows:

$$GL(x; F, E, m) = \frac{\exp(-4\ln 2(1-m)(x-E)^2/F^2)}{1 + 4m(x-E)^2/F^2} \tag{1}$$

with F denoting the full width at half maximum (FWHM) of the peak, E the position of the peak maximum, and m the relative fraction of Lorentzian shape of the peak. The outcome GL represents the normalized intensity of the peak at a given binding energy x. The described product form for constructing Voigt approximation is often used for practical PES peak fitting [21].

To elucidate the In 3d core-level line shape further, we tested also fittings according to previously calculated surface core-level shifts (SCLSs) for InAs, InSb and InP. After the background subtraction, a group of Gaussian-Lorentzian (Voigt) peaks corresponding to the different atomic sites described in previous reports [19, 20] were included in the fittings. Peaks with or under 0.05 eV separation from the bulk peak were not fitted, as the significant contribution and more trustworthy results come from adjusting the furthest components. It is worth noting that the presented fitting using the calculated shifts as the input parameters is different from the traditional target to resolve the minimum number of components of the measured spectrum. In contrast, here the fitting provides a test for the current
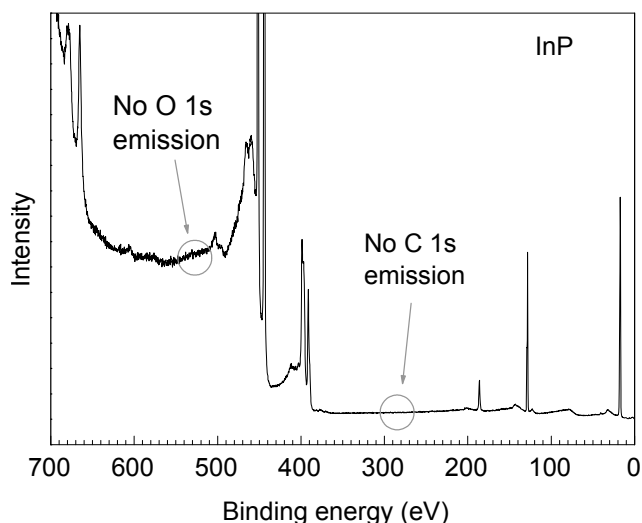
Figure 1: Survey spectrum measured from InP(100) after the cleaning procedure. Oxygen and carbon are below detectable limits.

atomic models as well. This approach is similar to that used previously [20].

The position of the bulk peak was not restricted. In contrast, the SCLSs were fixed: the previously calculated values for SCLSs were used as the input parameters. The Lorentzian and Gaussian peak contributions were allowed to vary. Physically reasoned restrictions were used: The intensity of the bulk peak was not allowed to grow for more surface sensitive measurements and also the bulk peak FWHM was fixed to lower values than the FWHMs of SLCS peaks that were fixed to have the same values together. Relevant peak parameters are listed in Table 1.

3. Results and discussion

Figure 1 illustrates a 700 to 0 eV survey spectrum measured from InP(100) after the cleaning procedure. The absence of detectable oxygen and carbon indicates an atomically clean surface, which justifies the fitting of In $3d_{5/2}$ without additional chemical shifts.

The In $3d_{5/2}$ emissions were first fitted by single peaks in order to analyze overall peak shapes, in particular, the contradictory high binding-energy side. We would still emphasize that the hypothesis was that these single peak fittings could not reproduce the spectra in detail, because of the natural surface reconstruction of these crystals. For optimal single peak fittings, we found the Lorentzian peak contribution of 60 to 83 % and the Gaussian one of 17 to 40 %, varying between the samples. It can be seen from Fig. 2 that the single peak fits best into In 3d of InSb, and the fit residual error between the spectrum and fitting increases slightly from inspection of the spectra for InGaAs and InAs to InP. Furthermore, it can be seen that the residual error appears on the low binding energy rather than on the high binding-energy side, consistent with that a semiconductor surface reconstruction usually causes a shift(s) on the low binding-energy side. The normalized residual between the fitted peak and measured values is close to 4 % for InP in wide areas of the spectrum whereas the residual is mostly below 2 % for the other samples. Given
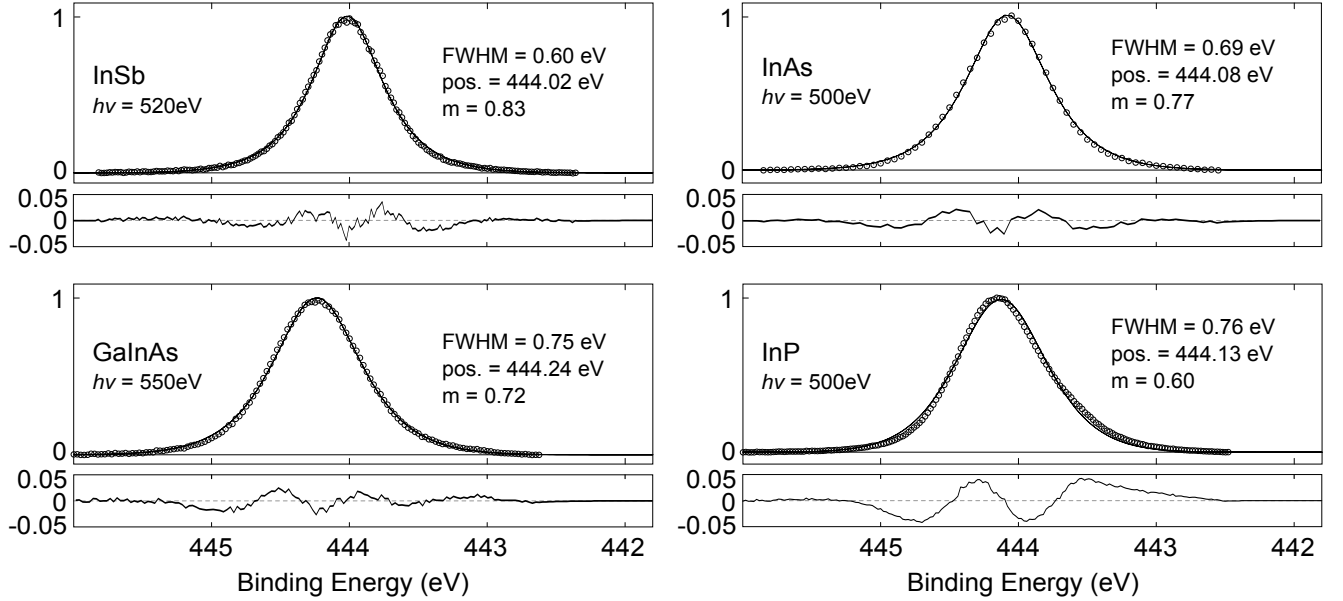
4

Figure 2: In 3d$_{5/2}$ photoelectron emissions with the excitation photon energy of about 500 eV for the investigated III-V samples fitted with a single symmetric Voigt peak approximation (solid line) to the measured data (open circles). Residuals between measured data and peak fits are plotted below each spectrum.

the lack of detectable contamination that would give rise to chemical shifts, this fitting error is likely due to different reconstructions and thus different SCLSs of the III-V surfaces, as the slight asymmetricity is clearly observed as a tail-like feature on the low binding energy side of InP. Indeed, InP(100) has the (2×4) reconstruction, which is clearly different from the (4×2) or c(8×2) structure on InAs(100), InGaAs(100) and InSb(100). It is worth noting that no (4×2) or c(8×2) appears on InP(100). Also, there is a difference between InAs and InSb surfaces because the pure ζa structure describes well InAs(100) while the mixture of the ζa and ζ structures appears on the InSb(100) surface [20] (see insets in Figures 3 and 4).

In addition to the surface reconstructions, In-droplets can readily form on InP-surface due to the Ar-sputtering [22–24]. The presence In-droplets with a metallic chemical environment is observed with a 0.5–0.8 eV separation from the bulk InP peak on the low binding energy side [23, 25].

Figures 3 and 4 show that the previously simulated SCLSs explain the In 3d emission for InAs(100) and InSb(100), supporting also these atomic models, as the components with largest separation give reasonable contributions to the spectral envelope, and minimize the fitting residual. For InP(100), In 3d emission can be characterized using SCLSs and a separate In 3d component for metallic In clusters as illustrated in Fig. 5. It is worth noting that including only the InP SCLSs in the fitting improved the residual significantly, as compared to the single peak fitting, similarly to the InAs and InSb cases. From these results it can be seen that the band gap of the III-V material does not cause tail-like distribution in the spectrum, as the spectra of the samples with different band gaps were successfully characterized using only symmetric peaks. For simplicity, the metallic In component was also characterized with a symmetric peak
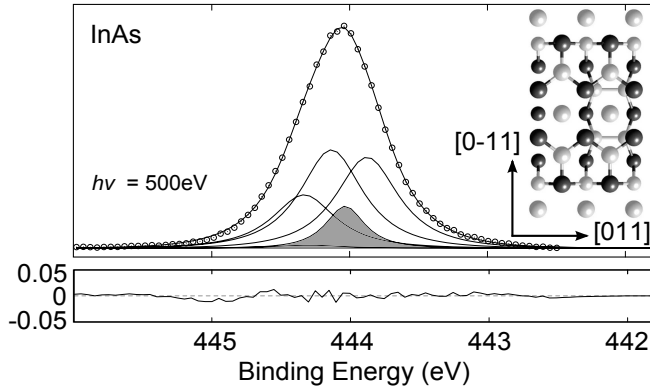
Figure 3: In 3d$_{5/2}$ emission measured with 500 eV photon energy from InAs(100). Unfilled circles represent the measured spectra and solid lines fitted and envelope peaks. The bulk peak is highlighted with gray color. Fitting was carried out utilizing SCLSs found for an InAs(100)c(8×2) ζa surface structure [20]. Residual for the spectral envelope fit is shown at the bottom. Inset: white spheres represent group III and dark spheres group V atoms.

shape because the asymmetry parameter is quite low ($\alpha \approx 0.02$), resulting in no significant changes in the envelope spectrum [24]. It was found that highly Lorentzian shaped peaks (of about 90 % Lorentzian and hence 10 % Gaussian) gave the best fits. The Lorentzian peak shape arises from the fact that the In 3d$_{5/2}$ energy level is quite deep, resulting in a short lifetime of the excited state and hence a broad FWHM which is Lorentzian rather than Gaussian in nature. Also, the Gaussian broadening can be low due to high-resolution instruments and well-ordered surface structures.

In Figures 4 and 5, the spectra for InP and InSb measured with the photon energies of around 500 eV (kinetic energy around 50 eV) are presented and provide the most surface sensitive measurements. The relative intensities of the bulk peaks for InSb were 6.8 %, 3.4 %, and 3.4 % for the measurements with the respective photon energies 600 eV, 520 eV, and 480 eV. For InP, the corresponding readings were 12.1 %, 11.8 %, 5.9 %, and 5.1 % for the measurements with photon energies 744 eV, 594 eV, 500 eV, 490 eV, respectively. The corresponding metallic droplet In intensities were 4.6 %, 6.1 %, 15.4 %, and 18.3 %. The decrease in the bulk peak intensity is consistent with an increase in the surface sensitivity of measurements.

Our observations for the SLCS fitting are also supported by the fact that the least surface sensitive measurements (744 eV for InP and 600 eV for InSb) give the most narrow peak shapes. Furthermore, the use of asymmetric tail-like line shapes, such as Doniach-Sunjic, would include background features in the high binding energy side of the peak, which is in contradiction with the presented results.

4. Conclusions

In summary, the high-resolution synchrotron-radiation CLPES results give a clear evidence that the asymmetric high-binding energy tail of In 3d$_{5/2}$ peaks is absent for pure In-containing III-V crystals. We have also shown that the sum of the symmetric Voigt-like peaks arising from the intrinsic surface reconstructions explains the observed spectral
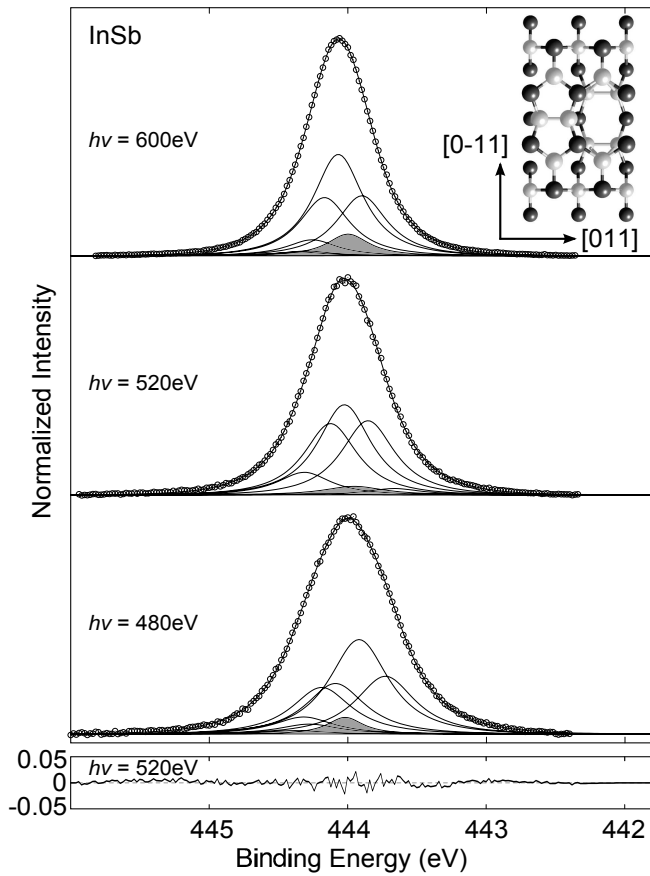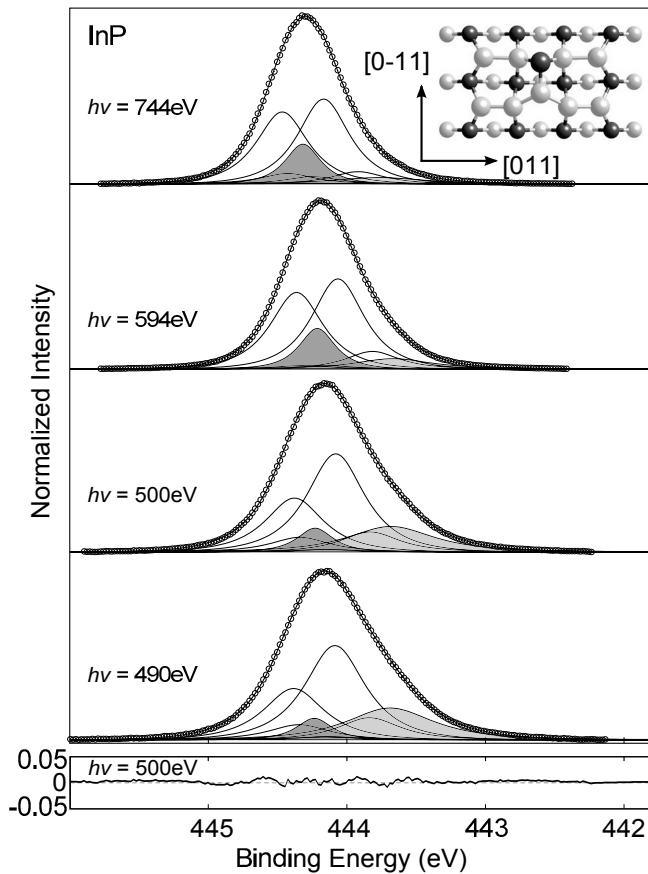
Figure 4: In 3d$_{5/2}$ emissions measured with various photon energies from InSb(100). Unfilled circles represent the measured spectra and solid lines fitted and envelope peaks. The bulk peak is highlighted with gray color. Fitting was carried out utilizing SCLSs found for an InSb(100)c(8×2) ζ surface structure [20]. Residual for the $h\nu$ = 520 eV spectral envelope fit is shown at the bottom. Inset: white spheres represent group III and dark spheres group V atoms.

Figure 5: In $3d_{5/2}$ emissions measured with various photon energies from InP(100). Unfilled circles represent the measured spectra and solid lines fitted and envelope peaks. Bulk and metallic indium peaks are highlighted with darker and lighter gray, respectively. Fitting was carried out utilizing SCLSs found for a mixed dimer InP(100)(2×4) surface structure [19]. Residual for the $h\nu$ = 500 eV spectral envelope fit is shown at the bottom. Inset: white spheres represent group III and dark spheres group V atoms.

features in detail. The dominance of the Lorentzian peak shape over the Gaussian one has been observed for In 3d. The results are helpful in the research and development of the In-containing III-V crystals for various applications.

Acknowledgements

References

[1] S. Oktyabrsky, P. Ye, Fundamentals of III-V Semiconductor MOSFETs, Springer, 2010.

[2] C. Hinkle, M. Milojevic, B. Brennan, A. Sonnet, F. Aguirre-Tostado, G. Hughes, E. Vogel, R. Wallace, Detection of Ga suboxides and their impact on III-V passivation and Fermi-level pinning, Appl. Phys. Lett. 94 (2009) 162101.

[3] C. Hinkle, E. Vogel, P. Ye, R. Wallace, Interfacial chemistry of oxides on $In_xGa_{(1-x)}As$ and implications for MOSFET applications, Curr. Opin. Solid State Mater. Sci. 15 (2011) 188 – 207.

[4] B. Shin, D. Choi, J. S. Harris, P. C. McIntyre, Pre-atomic layer deposition surface cleaning and chemical passivation of (100) $In_{0.2}Ga_{0.8}As$ and deposition of ultrathin Al_2O_3 gate insulators, Appl. Phys. Lett. 93 (2008) 052911–052911.

[5] R. Galatage, H. Dong, D. Zhernokletov, B. Brennan, C. Hinkle, R. Wallace, E. Vogel, Effect of post deposition anneal on the characteristics of HfO_2/InP metal-oxide-semiconductor capacitors, Appl. Phys. Lett. 99 (2011) 172901.

[6] C. Wang, S. Wang, G. Doornbos, G. Astromskas, K. Bhuwalka, R. Contreras-Guerrero, M. Edirisooriya, J. Rojas-Ramirez, G. Vellianitis, R. Oxland, et al., InAs hole inversion and bandgap interface state density of 2×10^{11} cm^{-2} eV^{-1} at HfO_2/InAs interfaces, Appl. Phys. Lett. 103 (2013) 143510.

[7] M. Passlack, S.-W. Wang, G. Doornbos, C.-H. Wang, R. Contreras-Guerrero, M. Edirisooriya, J. Rojas-Ramirez, C.-H. Hsieh, R. Droopad, C. H. Diaz, Lifting the off-state bandgap limit in InAs channel metal-oxide-semiconductor heterostructures of nanometer dimensions, Appl. Phys. Lett. 104 (2014) 223501.

[8] A. Luque, S. Hegedus, Handbook of photovoltaic science and engineering, 2nd ed., John Wiley & Sons, 2011.

[9] J. Tommila, V. Polojärvi, A. Aho, A. Tukiainen, J. Viheriälä, J. Salmi, A. Schramm, J. Kontio, A. Turtiainen, T. Niemi, et al., Nanostructured broadband antireflection coatings on AlInP fabricated by nanoimprint lithography, Sol. Energy Mater. Sol. Cells 94 (2010) 1845–1848.

[10] J. Tommila, A. Aho, A. Tukiainen, V. Polojärvi, J. Salmi, T. Niemi, M. Guina, Moth-eye antireflection coating fabricated by nanoimprint lithography on 1 eV dilute nitride solar cell, Prog. Photovoltaics: Res. Appl. 21 (2013) 1158–1162.

[11] P. King, T. D. Veal, C. Kendrick, L. R. Bailey, S. M. Durbin, C. F. McConville, InN/GaN valence band offset: High-resolution x-ray photoemission spectroscopy measurements, Phys. Rev. B 78 (2008) 033308.

[12] L. Bailey, T. Veal, C. McConville, Stable passivation of InN surface electron accumulation with sulphur treatment, Phys. Status Solidi (c) 8 (2011) 1605–1607.

[13] A. Kirk, M. Milojevic, J. Kim, R. Wallace, An in situ examination of atomic layer deposited alumina/InAs (100) interfaces, Appl. Phys. Lett. 96 (2010) 202905.

[14] C. Hinkle, M. Milojevic, E. Vogel, R. Wallace, The significance of core-level electron binding energies on the proper analysis of InGaAs interfacial bonding, Appl. Phys. Lett. 95 (2009) 151905.

[15] B. Brennan, H. Dong, D. Zhernokletov, J. Kim, R. M. Wallace, Surface and Interfacial Reaction Study of Half Cycle Atomic Layer Deposited Al_2O_3 on Chemically Treated InP Surfaces, Appl. Phys. Express 4 (2011) 125701.

[16] D. Zhernokletov, H. Dong, B. Brennan, M. Yakimov, V. Tokranov, S. Oktyabrsky, J. Kim, R. Wallace, Surface and interfacial reaction study of half cycle atomic layer deposited HfO_2 on chemically treated GaSb surfaces, Appl. Phys. Lett. 102 (2013) 131602.

[17] J. F. Moulder, W. F. Stickle, P. E. Sobol, K. D. Bomben, Handbook of X-ray photoelectron spectroscopy, volume 40, Perkin Elmer Eden Prairie, MN, 1992.

[18] S. Doniach, M. Sunjic, Many-electron singularity in X-ray photoemission and X-ray line spectra from metals, J. Phys. C: Solid State Phys. 3 (1970) 285.

[19] M. P. Punkkinen, P. Laukkanen, M. Ahola-Tuomi, J. Pakarinen, M. Kuzmin, A. Tukiainen, R. Perälä, J. Lång, M. Ropo, K. Kokko, et al., Core-level shifts of InP(100)(2×4) surface: Theory and experiment, Surf. Sci. 603 (2009) 2664–2668.

[20] P. Laukkanen, M. Punkkinen, M. Ahola-Tuomi, J. Lång, K. Schulte, A. Pietzsch, M. Kuzmin, J. Sadowski, J. Adell, R. Perälä, et al., Core-level shifts of the c(8×2)-reconstructed InAs(100) and InSb(100) surfaces, J. Electron Spectrosc. Relat. Phenom. 177 (2010) 52–57.

[21] Casa Software Ltd., CasaXPS, Line Shapes, 2009. `http://www.casaxps.com/help_manual/line_shapes.htm`, accessed December 5, 2014.

[22] B. Gruzza, B. Achard, C. Pariset, Surface composition of (100) InP substrates bombarded by low energy Ar^+ ions, studied by AES and EPES, Surf. Sci. 162 (1985) 202–208.

[23] C. Robert-Goumet, G. Monier, B. Zefack, S. Chelda, L. Bideux, B. Gruzza, O. Awitor, SEM and XPS studies of nanohole arrays on InP(100) surfaces created by coupling AAO templates and low energy Ar^+ ion sputtering, Surf. Sci. 603 (2009) 2923–2927.

[24] J. Woll, T. Allinger, V. Polyakov, J. Schaefer, A. Goldmann, W. Erfurth, Electronic effects of surface In atoms at clean and hydrogenated InP(100) 4×2 surfaces, Surf. Sci. 315 (1994) 293–301.

[25] J. Vigneron, M. Herlem, E. Khoumri, A. Etcheberry, Cathodic decomposition of InP studied by XPS, Appl. Surf. Sci. 201 (2002) 51–55.